# Antillatoxin is a marine cyanobacterial toxin that potently activates voltage-gated sodium channels

**W. I. Li*, F. W. Berman*, T. Okino†, F. Yokokawa‡, T. Shioiri‡, W. H. Gerwick†, and T. F. Murray*§**

*Department of Physiology and Pharmacology, College of Veterinary Medicine, University of Georgia, Athens, GA 30602-7389; †College of Pharmacy, Oregon State University, Corvallis, OR 97331; and ‡Faculty of Pharmaceutical Sciences, Nagoya City University, Tanabe-dori, Mizuho-ku, Nagoya 467-8603, Japan

Edited by John W. Daly, National Institutes of Health, Bethesda, MD, and approved April 9, 2001 (received for review February 20, 2001)

**Antillatoxin (ATX) is a lipopeptide derived from the pantropical marine cyanobacterium *Lyngbya majuscula*. ATX is neurotoxic in primary cultures of rat cerebellar granule cells, and this neuronal death is prevented by either *N*-methyl-D-aspartate (NMDA) receptor antagonists or tetrodotoxin. To further explore the potential interaction of ATX with voltage-gated sodium channels, we assessed the influence of tetrodotoxin on ATX-induced $Ca^{2+}$ influx in cerebellar granule cells. The rapid increase in intracellular $Ca^{2+}$ produced by ATX (100 nM) was antagonized in a concentration-dependent manner by tetrodotoxin. Additional, more direct, evidence for an interaction with voltage-gated sodium channels was derived from the ATX-induced allosteric enhancement of [$^3$H]batrachotoxin binding to neurotoxin site 2 of the $\alpha$ subunit of the sodium channel. ATX, moreover, produced a strong synergistic stimulation of [$^3$H]batrachotoxin binding in combination with brevetoxin, which is a ligand for neurotoxin site 5 on the voltage-gated sodium channel. Positive allosteric interactions were not observed between ATX and either $\alpha$-scorpion toxin or the pyrethroid deltamethrin. That ATX interaction with voltage-gated sodium channels produces a gain of function was demonstrated by the concentration-dependent and tetrodotoxin-sensitive stimulation of $^{22}Na^+$ influx in cerebellar granule cells exposed to ATX. Together these results demonstrate that the lipopeptide ATX is an activator of voltage-gated sodium channels. The neurotoxic actions of ATX therefore resemble those of brevetoxins that produce neural insult through depolarization-evoked $Na^+$ load, glutamate release, relief of $Mg^{2+}$ block of NMDA receptors, and $Ca^{2+}$ influx.**

Marine cyanobacteria represent a particularly rich source of structurally unique neurotoxic secondary metabolites (1–5). *Lyngbya majuscula* is a pantropical marine cyanobacterium that is the source of antillatoxin (ATX), a structurally unusual lipopeptide (1) (Fig. 1). Blooms of *L. majuscula* have been associated with adverse effects on human health. These blooms have been reported to cause respiratory irritation, eye inflammation, and severe contact dermatitis in exposed fishermen and swimmers (6). ATX has been shown to be among the most ichthyotoxic metabolites isolated to date from a marine microalga (1) and, more recently, has been demonstrated to be neurotoxic in primary cultures of rat cerebellar granule cells (4). In the latter study, morphologic evidence of ATX-induced neurotoxicity included swelling of neuronal somata, thinning of neurites, and blebbing of neurite membranes. ATX also induced a concentration-dependent cytotoxicity in cerebellar granule neurons as monitored by lactate dehydrogenase efflux (ATX $EC_{50} = 20.1 \pm 6.4$ nM) (4). This neurotoxic response of ATX was prevented by coexposure with noncompetitive antagonists of the *N*-methyl-D-aspartate (NMDA) receptor such as MK-801 and dextrorphan.

Voltage-gated sodium channels are responsible for generation of the rising phase of the action potential in membranes of neurons as well as in most other electrically excitable cells. Sodium channels consist of a pore-forming $\alpha$ subunit of 260 kDa associated with auxiliary $\beta$ subunits of 33–36 kDa (7, 8). Voltage-gated sodium channels represent the molecular target for an array of natural products including marine neurotoxins. Marine neurotoxins such as tetrodotoxin (TTX), saxitoxin, conotoxins, sea anemone toxins, brevetoxin, and ciguatoxin all bind with high affinity and specificity to at least six distinct receptor sites on sodium channel $\alpha$ subunits (8). Collectively, these toxins have served as important tools to explore the structure and function of voltage-dependent sodium channels. These marine neurotoxins produce characteristic alterations in the two major properties of sodium channels, namely ion permeation and gating (8).

The objective of the present study was to test the hypothesis that ATX acts as an activator of voltage-dependent sodium channels. This hypothesis emanated from our previous studies which were consistent with ATX acting as an autocrine excitotoxic agent in cerebellar granule neurons. In this study we have used a combination of neurochemical and pharmacological approaches to show that ATX is a structurally unusual lipopeptide activator of neuronal voltage-gated sodium channels.

## Materials and Methods

**Materials.** Tritiated batrachotoxin A 20-$\alpha$-benzoate ([$^3$H]BTX) and $^{22}Na^+$ were obtained from DuPont/NEN. Deltamethrin was purchased from Biomol (Plymouth Meeting, PA). Veratridine, brevetoxin-1 (PbTx-1), and ouabain were obtained from Sigma. Sea anemone toxin was purchased from Calbiochem. Fluo-3 AM and pluronic acid were obtained from Molecular Probes. ATX was either authentic natural (−)-antillatoxin, isolated as described (1), or synthetic (−)-antillatoxin prepared as published (2, 3). All other chemicals were reagent grade from commercial sources.

**Cerebellar Granule Cell (CGC) Culture.** Primary cultures of CGCs were obtained from 8-day-old Sprague–Dawley rats by a previously described method (9). Cerebella were removed, stripped of their meninges, minced by mild trituration with a Pasteur pipette, and treated with trypsin for 15 min at 37°C. The cells were then dissociated by two successive trituration and sedimentation steps in soybean trypsin inhibitor- and DNase-containing isolation buffer, centrifuged, and resuspended in basal Eagle's medium with Earle's salts containing 10% heat-inactivated FBS, 2 mM glutamine, 25 mM KCl, and 100 $\mu$g/ml gentamicin. CGCs were plated onto poly-L-Lysine (molecular weight = 393,000)-coated, 96-well (9-mm), clear-bottomed, black-well culture plates (Costar) at a density of $9.6 \times 10^4$ cells per well and 6-well (35-mm) culture dishes (Fisher) at a density of $2.5–2.75 \times 10^6$ cells per well, respectively, and incubated at 37°C in a 5% $CO_2$/95% humidity atmosphere. Cytosine arabinonucleoside

PHARMACOLOGY

This paper was submitted directly (Track II) to the PNAS office.

Abbreviations: ATX, antillatoxin; NMDA, *N*-methyl-D-aspartate; [$^3$H]BTX, tritiated batrachotoxin A 20-$\alpha$-benzoate; PbTx-1, brevetoxin 1; CGC, cerebellar granule cell; TTX, tetrodotoxin; $[Ca^{2+}]_i$, intracellular $Ca^{2+}$ concentration.

§To whom reprint requests should be addressed. E-mail: tmurray@vet.uga.edu.

The publication costs of this article were defrayed in part by page charge payment. This article must therefore be hereby marked "*advertisement*" in accordance with 18 U.S.C. §1734 solely to indicate this fact.

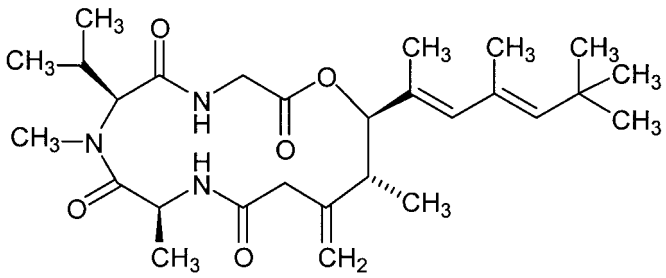


**Fig. 1.** Chemical structure of natural (−)-antillatoxin, which is composed of a tripeptide that forms both ester and amide linkages with a highly methylated lipid section.

(10 $\mu$M final concentration) was added after 18–24 h to inhibit replication of nonneuronal cells. Cells were fed after 7 days in culture with 50 $\mu$l/ml of a 25-mg/ml glucose solution.

**Cytotoxicity Assays.** CGCs were used for cytotoxicity assays at 10–13 days in culture. All assays were carried out in 1% DMSO, which by itself had no effect on neurons. Growth medium was collected and saved, and CGCs were washed twice in 1 ml of Locke's incubation buffer. CGCs were then exposed to ATX in the presence or absence of TTX for 2 h at 22°C. At the termination of exposure, the incubation medium was collected for later analysis of lactate dehydrogenase activity by using the method of Koh and Choi (12).

**Intracellular $Ca^{2+}$ Monitoring.** CGCs grown in 96-well plates were used for intracellular $Ca^{2+}$ concentration ($[Ca^{2+}]_i$) measurements at 10–13 days in culture as described (9). Briefly, the growth medium was removed and replaced with dye loading medium (100 $\mu$l per well) containing 4 $\mu$M fluo-3 AM and 0.04% pluronic acid in Locke's buffer (154 mM NaCl/5.6 mM KCl/1.0 mM $MgCl_2$,/2.3 mM $CaCl_2$/8.6 mM Hepes/5.6 mM glucose/0.1 mM glycine, pH 7.4). After 1 h of incubation in dye loading medium, the neurons were washed four times in fresh Locke's buffer (200 $\mu$l per well, 22°C) by using an automated cell washer (Thermo Labsystems, Helsinki, Finland) and transferred to the fluorescent laser imaging plate reader (Molecular Devices) incubation chamber. The final volume of Locke's buffer in each well was 100 $\mu$l.

The fluorescent laser imaging plate reader operates by illuminating the bottom of a 96-well microplate with an argon laser and measuring the fluorescence emissions from cell-permeant dyes in all 96 wells simultaneously by using a cooled charge-coupled device camera (13). In all experiments, antagonist compounds were added to the neurons from one source plate in a 50-$\mu$l volume at a rate of 10 $\mu$l/s 3 min before the addition of a 50-$\mu$l volume of ATX added from the second source plate at 25 $\mu$l/s, yielding a final volume of 200 $\mu$l per culture well with 1% DMSO. Neurons were excited by the 488-nm line of the argon laser, and $Ca^{2+}$-bound fluo-3 emission in the 500- to 560-nm range was recorded by the charge-coupled device camera with shutter speed set at 0.4 s. Fluorescence readings were taken once every 2 s for 10 s before antagonist additions, every 10 s during the 3 min before ATX addition, then once per s for 75 s after ATX exposure, and every 30 s thereafter until the programmed termination of the experiment. Background fluorescence was automatically subtracted from all fluo-3 fluorescence measurements.

**Whole Cell Binding Assay.** At 10–13 days in culture, CGCs cultured in six-well plates were used for measurement of [$^3$H]BTX binding. Cells were first rinsed three times each with 2 ml of buffer A containing 140 mM choline chloride, 5 mM KCl, 1.8 mM $CaCl_2$, 0.8 mM $MgSO_4$, and 10 mM Hepes (pH 7.4 with 1 M Tris). Cells were then incubated with buffer B (buffer A plus 2 mg/ml BSA) containing vehicle (DMSO) or various compounds. Except for the time course experiments in which the incubation time was varied, all whole cell binding assays were incubated for 3–4 h. After incubation, CGCs were rinsed three times with 2 ml of buffer A before lysis with 1 ml of 1% Triton X-100 under a condition of constant shaking overnight. A 750-$\mu$l aliquot of the resulting lysate was collected, and [$^3$H]BTX bound was measured by liquid scintillation counting. Nonspecific binding of [$^3$H]BTX was determined as [$^3$H]BTX bound in the presence of 100 $\mu$M veratridine. Our preliminary results indicated that whole cell assays conducted at room temperature (22°C) provided an optimum signal-to-noise ratio; all binding experiments reported herein were therefore conducted at 22°C.

**Measurement of $^{22}Na^+$ Influx.** CGCs were cultured in Falcon 3001 tissue culture dishes (35 mm) and used for experiments at 7–11 days in culture. CGCs were first rinsed three times each with a 2-ml preincubation solution containing 150 mM choline chloride, 5.6 mM KCl, 1 mM $MgCl_2$, 2.3 mM $CaCl_2$, 8.6 mM Hepes (pH 7.4, adjusted with Tris base), and 5.6 mM glucose. After these rinses, CGCs were incubated in a solution containing 145 mM choline, 5.6 mM KCl, 1 mM $MgCl_2$, 2.3 mM $CaCl_2$, 8.6 mM Hepes, 5 mM NaCl, 2 mM ouabain, and 0.25 $\mu$Ci of $^{22}Na^+$ for specified times. The $Na^+$ influx was stopped by aspiration of incubation solution and rinsed three times each with 1 ml of the preincubation solution. CGCs were then lysed with 1 ml of 1% Triton X-100 under constant shaking overnight; 750 $\mu$l of the resulting lysate was collected, and $^{22}Na^+$ content was determined by liquid scintillation counting. $^{22}$Na influx experiments were conducted at room temperature (22°C).

**Analysis of Experimental Data.** All experiments were performed with triplicate determinations and repeated twice with different cultures. Data were analyzed by nonlinear least-square regression analysis using the commercially available PRISM software (Version 3.0, GraphPad Software, San Diego). For kinetic studies, a one-phase exponential association was used to analyze the half-time and rate of [$^3$H]BTX association. The parameters ($K_d$, $B_{max}$) of equilibrium saturation binding were derived by nonlinear regression analysis-based fitting of a hyperbolic equation to the data, whereas concentration–response data were fitted by a three-parameter logistic equation.

## Results

**TTX Prevents ATX-induced Cytotoxicity.** In a previous report we demonstrated that a 2-h exposure to ATX produced substantial neuronal losses in CGC in primary culture (4). We reasoned that ATX, like brevetoxin and domoic acid, may act as an autocrine excitotoxic agent in CGC by depolarizing these glutamatergic neurons and, as a consequence, evoke the release of glutamate (9, 10). This notion was based on the finding that NMDA receptor antagonists prevented ATX-induced cytotoxicity in CGC (2). This hypothesis was tested by assessing the influence of TTX on the neurotoxic effect of ATX. Exposure of neurons to 100 nM ATX for 2 h elevated lactate dehydrogenase release from 25.5 ± 3 to 709 ± 21 (units per plate) during a 24-h period. Coincubation of TTX (1 $\mu$M) with ATX (100 nM) during the 2-h exposure period eliminated ATX neurotoxicity as monitored by assaying lactate dehydrogenase activity in the exposure buffer (99.5 ± 25 units per plate). These data suggested that ATX-induced neurotoxicity may depend on the activation of voltage-gated sodium channels. In further support of the concept that ATX may act as a sodium channel toxin, we found that ATX produces a concentration-dependent increase in cell death in

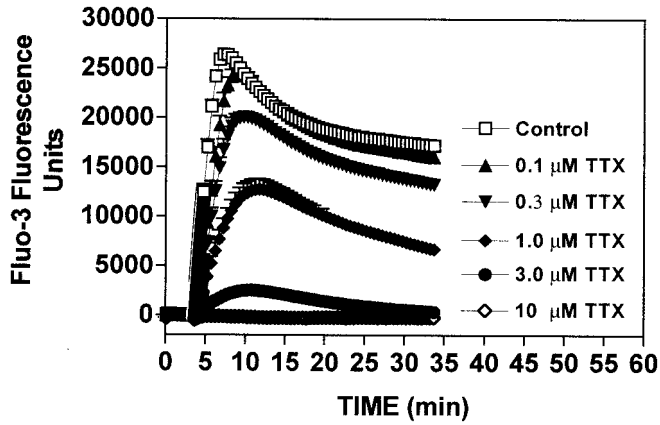


**Fig. 2.** Effect of treatment with increasing concentrations of TTX on $[Ca^{2+}]_i$ in CGCs exposed to 100 nM ATX. Buffer or TTX was added to neurons 3 min before the addition of ATX. The increase in fluo-3 fluorescence in response to ATX (100 nM) alone is depicted in the control curve. Data represent the mean ± SEM of three separate experiments performed in quadruplicate.

neuro-2a cells treated with ouabain and veratridine (data not shown).

**TTX Antagonizes ATX-induced $Ca^{2+}$ Influx in CGCs.** To further assess the involvement of voltage-gated sodium channels in the actions of ATX, we next examined the influence of ATX on $[Ca^{2+}]_i$ in CGCs. We have previously shown that activators of sodium channels such as brevetoxins trigger an influx of $Ca^{2+}$ in CGC that contributes to the cytotoxicity of these marine biotoxins (11). As shown in Fig. 2, ATX produced a rapid increase in $[Ca^{2+}]_i$ in CGCs. This response to ATX (100 nM), as monitored by fluo-3 fluorescence, peaked within 5–10 min and declined gradually to a plateau level. To ascertain the role of voltage-gated sodium channels in this response to ATX, we again determined the influence of TTX on the ATX-induced increase in $[Ca^{2+}]_i$. Pretreatment of neurons with TTX produced a concentration-dependent antagonism of the ATX-induced fluo-3 fluorescence response (Fig. 2). These results are consistent with the effects of TTX on the neurotoxicity of ATX and allow us to conclude that voltage-gated sodium channels may represent the molecular target for ATX.

**ATX Modulation of [$^3$H]BTX Binding to Voltage-Gated Sodium Channels in Intact CGCs.** [$^3$H]BTX is a radioligand probe that labels receptor site 2 on the voltage-gated sodium channel (14). This ligand binds preferentially to the active or open state of the channel, and the specific binding is sensitive to conformational changes induced by the binding of neurotoxins at other receptor sites on voltage-gated sodium channels. We have therefore used [$^3$H]BTX as a probe to provide direct evidence of ATX interaction with voltage-gated sodium channels.

The specific binding of [$^3$H]BTX to sodium channels in intact CGCs was quite low in the absence of other neurotoxins. As reported by others (14, 15), we found that neurotoxins acting at receptor sites 3, 5, and 7 (pyrethroid) enhanced [$^3$H]BTX-specific binding through allosteric interactions. As depicted in Fig. 3, the pyrethroid deltamethrin, PbTx-1, and sea anemone toxin all stimulated [$^3$H]BTX-specific binding over confined concentration ranges. These positive allosteric interactions verify the specificity of the specific binding of [$^3$H]BTX to voltage-gated sodium channels in CGC.

Similar to the positive allosteric action of deltamethrin, PbTx-1, and sea anemone toxin, ATX produced a concentration-dependent stimulation of [$^3$H]BTX-specific binding (Fig. 4). The ATX concentration–effect curve was leftward shifted in the presence of 100 nM PbTx-1, demonstrating the synergistic effects of ATX and PbTx-1 on the binding of [$^3$H]BTX to site 2. The $EC_{50}$ value for ATX stimulation of [$^3$H]BTX binding was 635 ± 60 nM in the absence and 50 ± 6 nM in the presence of PbTx-1. To further assess the interaction of ATX with neurotoxin site 3, 5, and 7 ligands, we evaluated the combination of maximally effective concentrations of PbTx-1, sea anemone toxin, and deltamethrin with ATX. ATX (100 nM) alone enhanced [$^3$H]BTX binding 4.8-fold, whereas 100 nM PbTx-1 produced a more modest 2-fold stimulation. The combination of ATX (100 nM) and PbTx-1 (100 nM) synergistically increased specific binding 16.6-fold above control values. Sea anemone toxin at a concentration of 300 nM produced a 1.8-fold increase in specific [$^3$H]BTX binding, and this was increased further to 4.6-fold in combination with ATX (100 nM). The fold increase observed with the combination of sea anemone toxin and ATX is equivalent to that seen with ATX alone, thereby indicating a lack of synergism between ATX and neurotoxin site 3. The pyrethroid deltamethrin (10 $\mu$M) produced a 2.2-fold enhancement of binding and, similar to sea anemone toxin, this was increased to 5.2-fold stimulation when combined with ATX (100 nM), which again is equivalent to the fold increase in the presence of ATX alone. The observation that ATX further enhances [$^3$H]BTX binding in the presence of maximally effective concentrations of either sea anemone toxin or deltamethrin suggests that these three ligands act at topologically distinct sites that are not allosterically coupled. In contrast, neurotoxin site 5 does appear to be allosterically coupled to the ATX site inasmuch as strong synergistic effects of ATX and PbTx-1 on [$^3$H]BTX binding were observed. This lack of coupling between the pyrethroid site and the ATX was further demonstrated by assessing the ability of deltamethrin to affect [$^3$H]BTX binding in the presence of ATX and PbTx-1 together. As depicted in Fig. 5, the binding of [$^3$H]BTX in the presence of the combination of ATX and PbTx-1



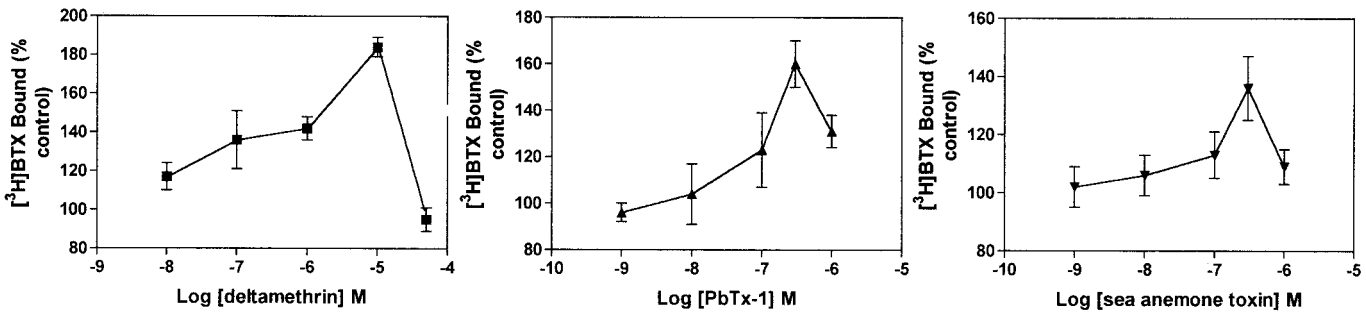


**Fig. 3.** Enhancement of the specific binding of [$^3$H]BTX (2 nM) to intact CGCs. Deltamethrin, PbTx-1, and sea anemone toxin all produced an allosteric stimulation of [$^3$H]BTX binding. Data represent the mean ± SEM from three experiments.

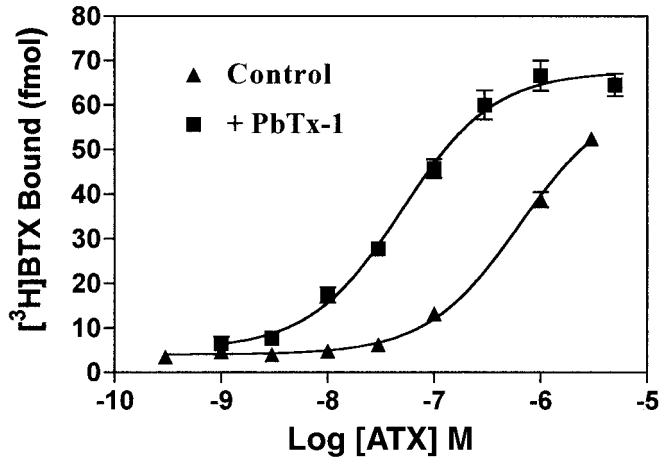


**Fig. 4.** ATX stimulation of [$^3$H]BTX (6 nM) specific binding in the presence and absence of PbTx-1 (100 nM). A three-parameter logistic fit to the experimental data yielded a control ATX $EC_{50}$ value of 635 ± 60 nM, which was leftward shifted to a value of 50 ± 6 nM in the presence of PbTx-1 (100 nM). Data shown are from a representative experiment performed in triplicate that was repeated twice.

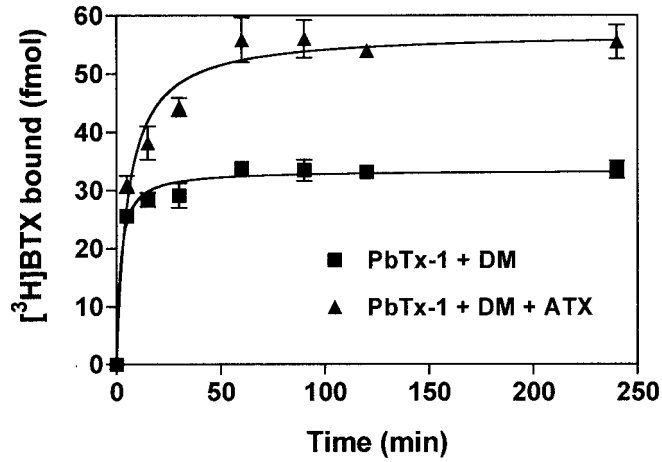


**Fig. 6.** Time course of the specific binding of [$^3$H]BTX (3 nM) to intact CGCs. [$^3$H]BTX association was determined in the presence of PbTx-1 (100 nM) and deltamethrin (DM, 10 $\mu$M), or the combination of PbTx-1, deltamethrin, and 100 nM ATX. ATX affects primarily the maximum level of [$^3$H]BTX binding and not the association rate. Data shown are derived from a representative experiment that was performed in triplicate and repeated twice.

was virtually identical to that observed in the presence of all three neurotoxins.

In the absence of ATX, the combination of PbTx-1 and deltamethrin afforded maximum signal-to-noise ratios. The association of [$^3$H]BTX specific binding in the presence of PbTx-1 and deltamethrin progressed rapidly with a $t_{1/2}$ of 2.3 ± 0.06 min, and equilibrium was attained at $t \geq 45$ min. The inclusion of ATX in this association reaction had little influence on the approach to equilibrium ($t_{1/2}$ = 6.0 ± 0.02 min) but greatly enhanced the level of specific [$^3$H]BTX bound at equilibrium (1.7-fold increase) (Fig. 6). This effect on equilibrium binding of [$^3$H]BTX was further examined through an assessment of the influence of ATX on [$^3$H]BTX equilibrium saturation binding. This analysis indicated that the [$^3$H]BTX $K_d$ value was 88.7 ± 6.7 nM in the presence of deltamethrin and PbTx-1, whereas the saturation isotherm was leftward shifted by the addition of ATX with the other neurotoxins, yielding a $K_d$ value of 30.4 ± 12.9 nM (Fig. 7). The $B_{max}$ values for [$^3$H]BTX binding to intact CGCs were not significantly affected (PbTx-1 + deltamethrin = 91.2 ± 12.8 fmol; PbTx-1 + deltamethrin + ATX = 78.7 ± 3.7 fmol). These data indicate that the ability of ATX to increase [$^3$H]BTX binding to site 2 of voltage-gated sodium channels is the result of an allosteric interaction that increases the affinity of this site for [$^3$H]BTX.

**ATX Stimulation of $^{22}Na^+$ Influx in Intact CGC.** Although the ability of ATX to enhance [$^3$H]BTX binding is consistent with an activation of voltage-gated sodium channels, we adapted the $^{22}Na^+$ flux assay described by Catterall and collaborators (16, 17) to CGCs in an effort to determine directly whether ATX interaction with this ion channel induces a gain of function.

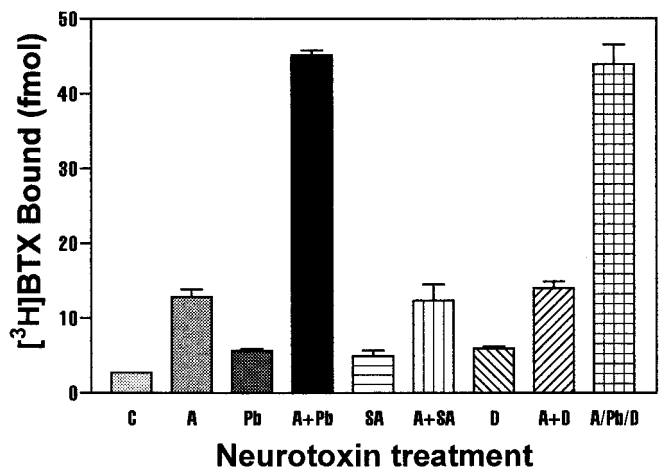


**Fig. 5.** Neurotoxin-induced enhancement of the specific binding of [$^3$H]BTX (5 nM) to intact CGCs. Neurotoxins tested (with abbreviations and concentration) in this experiment were as follows: control (C), ATX (A, 100 nM), PbTx-1 (Pb, 100 nM), sea anemone toxin (SA, 300 nM), and deltamethrin (D, 10 $\mu$M). All neurotoxins were tested alone and in combination with ATX (A). These data are from a representative experiment performed in triplicate and repeated three times.

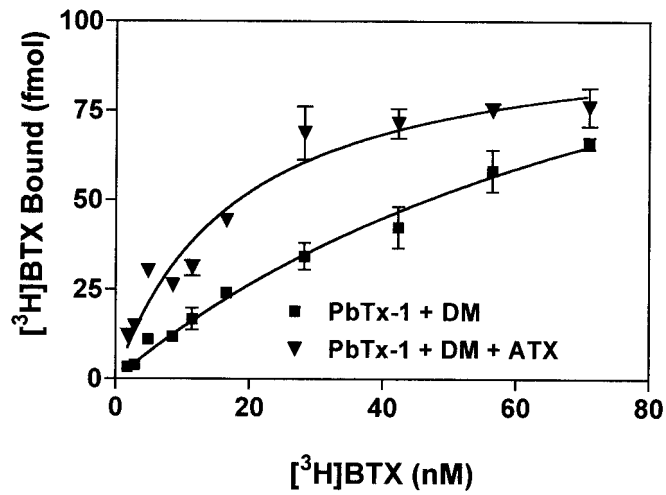


**Fig. 7.** ATX effect on equilibrium saturation binding of [$^3$H]BTX to intact cerebellar granule cells. Data depicted are mean ± SEM values of a representative experiment performed in duplicate that was repeated twice. The mean $K_d$ values for the three experiments show that ATX increases the affinity but not the $B_{max}$ of [$^3$H]BTX binding. In the presence of PbTx-1 and deltamethrin alone the $K_d$ = 88.7 ± 6.7 nM, whereas the addition of ATX shifted the $K_d$ to 30.4 ± 12.0 nM.

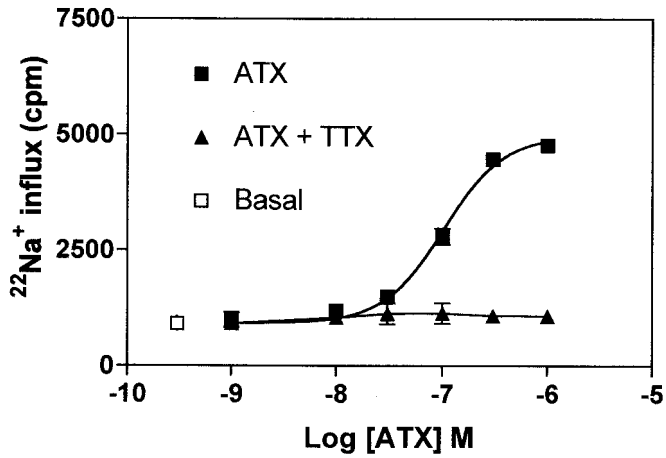


**Fig. 8.** Concentration–response curve for ATX stimulation of $^{22}Na^+$ influx in intact neurons. The 5-fold stimulation produced by ATX was prevented by the coapplication of 3 $\mu$M TTX. $^{22}Na^+$ influx was determined in CGCs incubated at 22°C for 5 min. Data shown are from a representative experiment performed in duplicate and repeated twice.

Preliminary studies indicated that both basal and neurotoxin-stimulated $^{22}Na^+$ influx were linear for 5 min in CGCs incubated at 22°C. The 5-min time point was therefore used in all subsequent experiments. As shown in Fig. 8, ATX elicited a concentration-dependent stimulation of $^{22}Na^+$ influx in CGCs. The $EC_{50}$ value for this response was 98.2 ± 12.0 nM, which is in agreement with the potency of ATX as an allosteric regulator of [$^3$H]BTX binding. To ensure that the observed $^{22}Na^+$ influx was mediated by voltage-gated sodium channels, we ascertained the influence of TTX on the response to ATX. Pretreatment of CGC with TTX (3 $\mu$M) abrogated ATX-induced $^{22}Na^+$ influx. These results provide strong support for the notion that ATX is an activator of voltage-gated sodium channels.

## Discussion

ATX is a lipopeptide that is structurally unique and characterized by a large number of methyl groups, including a rare *tert*-butyl group (1). Earlier studies showed ATX to be among the most potent ichthyotoxic compounds isolated from a marine alga (1). The ichthyotoxic potency is, in fact, exceeded only by PbTx-1 (1). It is also noteworthy that human inhalation exposure to *L. majuscula* produces symptoms such as respiratory irritation, which is also a salient feature of the toxic sequelae of aerosolized brevetoxin exposure from Florida and Texas red tides (6, 18).

Brevetoxins are potent lipid-soluble polyether neurotoxins produced by the marine dinoflagellate *Gymnodinium breve* (19). Brevetoxins are known to interact specifically with neurotoxin site 5 on the $\alpha$ subunit of voltage-gated sodium channel (19). This interaction with the $\alpha$ subunit causes a shift in the voltage dependence of channel activation to more negative potentials and inhibits channel inactivation, thereby producing neuronal depolarization at resting membrane potentials (20–25). Additional effects of brevetoxins on sodium channels are a 2-fold increase of the mean apparent channel open time at all membrane potentials and the appearance of subconductance states with distinct conductance levels (26, 27).

In CGCs a consequence of brevetoxin-induced depolarization is acute neuronal injury and cell death (10). This neurotoxic response can be prevented by coapplication of the sodium channel antagonist TTX or by NMDA receptor antagonists (10). The finding that brevetoxins evoke the release of glutamate from CGCs indicates that the neurotoxicity of these marine biotoxins is mediated by NMDA receptors that are activated indirectly as a consequence of brevetoxin activation of sodium channels with attendant excitatory amino acid release. Brevetoxins may therefore be viewed as capable of producing an autocrine excitotoxicity in CGCs.

In this latter sense brevetoxins are similar to another marine neurotoxin, domoic acid, which produces a neurotoxic response in CGCs that is mediated primarily by NMDA receptors (28). Again, domoic acid acts to produce autocrine excitotoxicity by activating $\alpha$-amino-3-hydroxy-5-methyl-4-isoxazolepropionic acid/kainate receptors that depolarize these neurons and trigger the release of glutamate. Thus, although domoic acid and brevetoxins interact with distinct molecular targets on CGCs, they both exert an autocrine excitotoxicity.

ATX-induced cytotoxicity resembles that of brevetoxin and domoic acid in that it may be prevented by coapplication of an NMDA receptor antagonist. The neurotoxic effect of ATX is, moreover, eliminated by TTX, thereby resembling the pattern observed with brevetoxin. Additional evidence consonant with the interaction of ATX with sodium channels is the concentration-dependent reversal of ATX-stimulated $Ca^{2+}$ influx in CGC by TTX. Analogous to the effect of brevetoxin on CGC (11), ATX evoked a rapid increase in $[Ca^{2+}]_i$ in CGCs that may derive from activation of voltage-dependent $Ca^{2+}$ channels, influx through NMDA receptors, and/or the reverse mode of operation of the $Na^+/Ca^{2+}$ exchanger (11). All of these pathways could be engaged as a consequence of ATX-induced activation of voltage-gated sodium channels with attendant depolarization and collapse of the sodium gradient.

To further explore the interaction of ATX with sodium channels, we used [$^3$H]BTX as a probe for neurotoxin site 2 on the $\alpha$ subunit of the channel. The specific binding of [$^3$H]BTX is sensitive to conformational changes induced by the binding of toxins to other sites on the $\alpha$ subunit (14). Hence, positive cooperativity between neurotoxin site 2 and 3 exists inasmuch as $\alpha$-scorpion toxin or sea anemone toxin binding to site 3 enhances the binding of [$^3$H]BTX to site 2 (14, 22). The binding of [$^3$H]BTX to neurotoxin site 2 is also enhanced by the interaction of the brevetoxin, PbTx-2, to neurotoxin site 5 on this $\alpha$ subunit of the sodium channel (22). The PbTx-2 stimulation of [$^3$H]BTX binding is synergistically enhanced by $\alpha$-scorpion toxin interaction with site 3 (22).

Synthetic pyrethroid insecticides such as deltamethrin and cypermethrin have been reported to increase the specific binding of [$^3$H]BTX to sodium channels (29). Pyrethroids shift the activation threshold to more negative membrane potentials and inhibit inactivation (30). Pyrethroids specifically bind to a site on the sodium channel $\alpha$ subunit that is distinct from neurotoxin site 1–6 and is allosterically coupled to sites 2, 3, and 5 (31, 32). The pyrethroid RU39568 has been shown to augment [$^3$H]BTX specific binding, and brevetoxin and $\alpha$-scorpion toxin further enhance this response (31).

In the present study we provide direct evidence for ATX interaction with a site on the $\alpha$ subunit of the sodium channel by using [$^3$H]BTX as a probe. ATX allosterically enhanced the specific binding of [$^3$H]BTX, and this was synergistically augmented by PbTx-1. In contrast to the synergistic interaction of ATX and brevetoxin, neither sea anemone toxin nor deltamethrin affected the ATX-induced enhancement of [$^3$H]BTX binding. These data indicate that the ATX site does not show positive cooperativity with neurotoxin site 3 or 7 (pyrethroid). This distinguishes the ATX site from site 5, the target for brevetoxin. The strong synergistic interaction of the ATX site with neurotoxin site 5 suggests that these sites may be topologically close and/or conformationally coupled. In the presence of PbTx-1 and deltamethrin, ATX increased the affinity of [$^3$H]BTX for site 2 by nearly 3-fold.

Considered together, the results obtained with [$^3$H]BTX allow us to exclude an interaction of ATX with neurotoxin sites 1, 2,

3, 5, and 7 on the sodium channel. Site 1 can be ruled out inasmuch as TTX and saxitoxin bind to the mouth of the pore of the ion channel and allosterically inhibit the binding of [$^3$H]BTX; sites 2 and 5 are ruled out because of the positive cooperativity between ATX and these sites; and sites 3 and 7 are eliminated inasmuch as ATX enhances [$^3$H]BTX binding in the presence of the maximally effective concentrations of ligands that occupy sites 3 and 7. We are left with the possibilities of either ATX binding to a distinct site on the sodium channel $\alpha$ subunit or an interaction of ATX with site 4, which we could not test because of the lack of commercially available $\beta$-scorpion toxin. The relatively small lipotripeptide structure of ATX would not, however, be restricted to an extracellular recognition domain as is the case for $\beta$-scorpion toxin.

The results presented herein that ATX can stimulate $Na^+$ influx in intact neurons in a TTX-sensitive manner confirms the suggestion that ATX is a previously unrecognized activator of voltage-gated sodium channels. The gain of function of voltage-gated sodium channels induced by ATX binding provides insight into the neurotoxic actions of this lipopeptide. Sodium channel activators such as the site 5 ligand, brevetoxin, produce neuronal injury in CGCs through depolarization-evoked $Na^+$ load, glutamate release, relief of $Mg^{2+}$ block of NMDA receptors, and $Ca^{2+}$ influx (10, 11). It is therefore reasonable to posit that the neurotoxic actions of ATX in CGCs share a common ensemble of underlying mechanisms, inasmuch as NMDA receptor antagonists are neuroprotective against both brevetoxin and ATX.

Further investigation will be required to define the recognition site for ATX on voltage-gated sodium channels. An understanding of the binding site for this lipopeptide will provide additional information on the structure–function relationships of voltage-gated sodium channels. The development of antagonists of the ATX lipopeptide site may provide another means of blocking sodium channels and thereby a strategy for the discovery of anticonvulsant and neuroprotectant drugs.

We thank Roxanne Armstrong and Kelli Cumuze for outstanding technical assistance. This work was supported by the Marine Freshwater Biomedical Sciences Center of Oregon State University (Grant ES03850) and by the University of Georgia Research Foundation.

1. Orjala, J., Nagle, D. G., Hsu, V. L. & Gerwick, W. H. (1995) *J. Am. Chem. Soc.* **117,** 8281–8282.
2. Yokokawa, F., Fujiwara, H. & Shioiri, T. (1999) *Tetrahedron Lett.* **40,** 1915–1916.
3. Yokokawa, F., Fujiwara, H. & Shioiri, T. (2000) *Tetrahedron* **56,** 1759–1775.
4. Berman, F. W., Gerwick, W. H. & Murray, T. F. (1999) *Toxicon* **37,** 1645–1648.
5. Wu, M., Okino, T., Nogle, L. M., Marquez, B. L., Williamson, R. T., Sitachitta, N., Berman, F. W., Murray, T. F., McGough, K., Jacobs, R., *et al*. (2000) *J. Am. Chem. Soc.* **122,** 12041–12042.
6. Dennison, W. C., O'Neil, J. M., Duffy, E. J., Oliver, P. E. & Shaw, G. R. (1999) *Bull. Inst. Oceanogr. (Monaco)* **NS19,** 501–506.
7. Catterall, W. A. (2000) *Neuron* **26,** 13–25.
8. Cestele, S. & Catterall, W. A. (2000) *Biochimie (Paris)* **82,** 883–892.
9. Berman, F. W. & Murray, T. F. (1996) *J. Biochem. Toxicol.* **11,** 111–119.
10. Berman, F. W. & Murray, T. F. (1999) *J. Pharmacol. Exp. Ther.* **290,** 439–333.
11. Berman, F. W. & Murray, T. F. (2000) *J. Neurochem.* **74,** 1443–1451.
12. Koh, J. Y. & Choi, D. W. (1987) *J. Neurosci. Methods* **20,** 83–90.
13. Schroeder, K. L. & Neagle, B. G. (1996) *J. Biomol. Screen.* **1,** 75–80.
14. Catterall, W. A., Morrow, C. S., Daly, J. W. & Brown, G. B. (1981) *J. Biol. Chem.* **256,** 8922–8927.
15. Linford, N. J., Cantrell, A. R., Qu, Y., Scheuer, T. & Catterall, W. A. (1998) *Proc. Natl. Acad. Sci. USA* **95,** 13947–13952.
16. Catterall, W. A. (1975) *Proc. Natl. Acad. Sci. USA* **72,** 1782–1786.
17. Tamkun, M. M. & Catterall, W. A. (1981) *Mol. Pharmacol.* **19,** 78–86.
18. Fleming, L. E. & Baden, D. G. (1998) *White Paper for the Proceedings of the Texas Conference on Neurotoxic Shellfish Poisoning* (Univ. of Texas Marine Science Inst., Port Aransas, TX), pp. 27–34.
19. Baden, D. G. (1989) *FASEB J.* **3,** 1807–1817.
20. Catterall, W. A. & Gainer, M. (1985) *Toxicon* **23,** 497–504.
21. Poli, M. A., Mende, T. J. & Baden, D. G. (1986) *Mol. Pharmacol.* **30,** 129–135.
22. Sharkey, R. G., Jover, E., Couraud, F., Baden, D. G. & Catterall, W. A. (1987) *Mol. Pharmacol.* **31,** 273–278.
23. Edwards, R. A., Trainer, V. L. & Baden, D. G. (1992) *Mol. Brain Res.* **14,** 64–70.
24. Rein, K. S., Baden, D. G. & Gawley, R. E. (1994) J. *Org. Chem.* **59,** 2101–2106.
25. Rein, K. S., Lynn, B., Gawley, R. E. & Baden, D. G. (1994) *J. Org. Chem.* **59,** 2107–2113.
26. Gawley, R. E., Rein, K. S., Jeglitsch, G., Adams, D. J., Theodorakis, E. A., Tiebes, J., Nicolaou, K. C. & Baden, D. G. (1995) *Chem. Biol.* **2,** 533–541.
27. Jeglitsch, G., Rein, K., Baden, D. G. & Adams, D. J. (1998) *J. Pharmacol. Exp. Ther.* **284,** 516–525.
28. Berman, F. W. & Murray, T. F. (1997) *J. Neurochem.* **69,** 693–703.
29. Brown, G. B., Gaupp, J. E. & Olsen, R. W. (1988) *Mol. Pharmacol.* **34,** 54–59.
30. Strichartz, G., Rando, T. & Wang, G. K. (1987) *Annu. Rev. Neurosci.* **10,** 237–267.
31. Trainer, V. L., Moreau, E., Guedin, D., Baden, D. G. & Catterall, W. A. (1993) *J. Biol. Chem.* **268,** 17114–17119.
32. Trainer, V. L., McPhee, J. C., Boutelet-Bochan, H., Baker, C., Scheuer, T., Babin, D., Demoute, J. P., Guedin, D. & Catterall, W. A. (1997) *Mol. Pharmacol.* **51,** 651–657.